THE NEAR ULTRAVIOLET ABSORPTION SPECTRUM OF GASEOUS HONO AND N_2O_3

WILLIAM R. STOCKWELL and JACK G. CALVERT

Chemistry Department, The Ohio State University, Columbus, Ohio 43210 (U.S.A.)

(Received August 3, 1977; in revised form October 10, 1977)

Summary

New measurements of the absorption cross sections for N_2O_3 and HONO vapors have been made for the 300 - 400 nm wavelength range. The N_2O_3 data were derived from the observed spectra of equilibrium mixtures of N_2O_3 with NO, NO_2 and N_2O_4. HONO data were derived from its equilibrium mixtures with NO, NO_2, H_2O, N_2O_3 and N_2O_4. Correction for the absorptions of NO_2 and N_2O_4 in the first mixtures and NO_2, N_2O_4 and N_2O_3 in the second mixtures were made using the measured initial compositions together with equilibrium and NO_2, N_2O_4 and N_2O_3 absorption cross section data. The measured cross sections for HONO(g) are significantly greater than those reported from similar experiments by Johnston and Graham and are somewhat smaller than those recently published by Cox and Derwent. The new data are consistent with relative rate measurements for the photochemical reactions $HONO + h\nu \rightarrow HO + NO$ and $NO_2 + h\nu \rightarrow O + NO$ studied in a simulated-sunlight-irradiated reaction chamber at low reactant concentrations. The first order rate constants for the first of these reactions in the lower atmosphere are estimated as 0.089, 0.088, 0.086, 0.083, 0.077, 0.068, 0.054, 0.035, 0.017 and 0.004 min^{-1} for sea level and no ground reflectivity with solar zenith angles of 0, 10, 20, 30, 40, 50, 60, 70, 78 and 86 °, respectively.

Introduction

In recent years there has been a renewed interest in the study of the gas phase reactions of HONO. This has been stimulated largely by two factors: (1) the need for a quantitative evaluation of the reaction pathways which form and destroy HONO in the atmosphere; (2) the increasing use of HONO as a convenient photochemical source of HO radicals in the laboratory.

The atmospheric chemistry of nitrous acid remains poorly defined today. Nash [1] seemingly identified HONO in the atmosphere of southern England (0.4 - 11 ppb), but the analytical method employed could, at best, provide

only a very indirect identification of this compound [2]. In theory nitrous acid is expected to be present in the NO_x–RH-polluted sunlight-irradiated atmosphere at levels in the range estimated by Nash. It may be formed in the atmosphere through several reaction pathways; for example, the following reactions have been considered in the computer simulation of the chemistry of the polluted atmosphere [3, 4]:

$$HO + NO (+M) \rightarrow HONO (+M) \tag{1}$$

$$HO_2 + NO_2 \rightarrow HONO + O_2 \tag{2}$$

$$NO + NO_2 + H_2O \rightarrow 2HONO \tag{3}$$

The ultimate concentration to which HONO will build is limited by the rates of its various removal reactions such as

$$2HONO \rightarrow NO + NO_2 + H_2O \tag{4}$$

$$HONO + HO \rightarrow H_2O + NO_2 \tag{5}$$

$$HONO + h\nu(\lambda < 400 \text{ nm}) \rightarrow HO + NO \tag{6}$$

Existing rate data suggest that reaction (6) is probably the dominant loss reaction for HONO in the atmosphere [4, 5], but the large difference between recent estimates of the absorption cross sections of HONO [6 - 8] make its rate uncertain by as much as a factor of 6. The methods used in the previous studies appear to be uncomplicated. In the HONO spectral studies of Johnston and Graham [7] nitrous acid was prepared by reactions (3) and (4), presumably at its equilibrium concentration, from starting gaseous mixtures of NO, NO_2 and H_2O in He. Corrections were made for absorptions due to NO_2, N_2O_4 and N_2O_3 in the spectrum. In the studies of HONO by Cox and Derwent [8], relatively pure dilute mixtures of HONO were prepared in a nitrogen carrier gas which was allowed to flow over an acidified nitrite salt solution. With this method corrections for NO_2 absorption were relatively small, and those due to N_2O_4 and N_2O_3 were negligible. In principle both of these recent quantitative studies of HONO absorption should provide reliable absorption cross section data, and it is not clear from the published information what problems led to the very different results. Obviously a further study of this system is necessary to establish the correct HONO absorption cross sections and to provide a more quantitative evaluation of the potential reactions of HONO in the atmosphere.

Cox has shown recently that nitrous acid vapors are an excellent photochemical source of HO radicals through reaction (6) [9 - 11]. Following his lead, we have studied some of the thermal and photochemical reactions of HONO vapors employing a Fourier transform spectroscopy (FTS) IR long-path spectroscopy system to follow HONO and various reactants and products [5, 12, 13]. In the course of these studies we observed that the rates of HONO photolysis were very much faster in dilute gaseous mixtures than we had anticipated from the measured intensities in our experiments at simulated solar intensities (290 - 410 nm region) and the HONO absorption

cross section data then available [7]. The present spectral study of HONO was initiated at that time in an attempt to re-evaluate the near UV absorption cross sections of HONO and to allow an unambiguous and independent check on our measured rates of reaction (6) in the reaction chamber. We utilized the equilibrium method employed by Johnston and Graham [7]. As our work neared completion, the recent study of Cox and Derwent [8] appeared. The new results which we report here are in qualitative accord with those reported by Cox and Derwent, although some significant differences appear.

Experimental

Spectral measurements of the gaseous mixtures of HONO, NO_2, N_2O_3, N_2O_4, NO and H_2O were made using a Cary 17 UV–visible spectrophotometer in a 10 cm path gas cell equipped with a Teflon vacuum stopcock and Supracil windows. The optical resolution varied with wavelength but was kept to less than 1 nm in the 325 - 450 nm range and to less than 5 nm in the 300 - 325 nm range. Since King and Moule [6] found no trace of fine structure in the HONO spectrum when they employed a 20 ft grating spectrograph with a resolving power of 150 000, our equipment was sufficient to resolve the structure of the HONO. The reactant gases NO and NO_2 (Matheson) and H_2O were purified by fractional distillation and degassing in two conventional high vacuum systems which were equipped with Teflon high vacuum stopcocks, calibrated volumes, pressure gauges and a quartz spiral manometer.

In the study of the N_2O_3 spectra, small quantities (1 - 14 Torr) of an NO_2-N_2O_4 gaseous mixture were added to the cell. Then a large measured quantity of NO (112 - 753 Torr) was introduced into the cell. The cell contents were allowed to equilibrate for about 30 min, and then the absorption spectrum of the mixture (300 - 450 nm) was determined. The NO_2 pressure in the cell was estimated from the visible absorption at 430, 440 and 448 nm using the absorption cross section data for these wavelengths reported by Hall and Blacet [14]; the three independent estimates of the $P(NO_2)$ checked well with one another, usually within a few per cent. From the measured $P(NO_2)$ in the equilibrium mixture and the $P^0(NO)$, $P(N_2O_4)$ and $P(N_2O_3)$ were calculated using the known equilibrium constants K_7 and K_8 for the given temperature of the particular experiment:

$$2NO_2 \rightleftharpoons N_2O_4 \tag{7}$$

$$NO + NO_2 \rightleftharpoons N_2O_3 \tag{8}$$

The values of K_7 and K_8 which we employed were derived from the JANAF enthalpy, entropy and heat capacity data [15] and should be reliable for temperatures used in this work (24 - 30 °C):

$$K_7 = \exp\{6989T^{-1} + 0.791 \ln(T/298) - 21.52\} \tag{9}$$

$$K_8 = \exp\{4834T^{-1} - 0.144 \ln(T/298) - 16.854\} \tag{10}$$

These expressions yield estimates which are in reasonable accord with the measured values of K_7 and K_8 at 298 K [16, 18] and 300 K [17]. The absorption data of Bass *et al.* [19] were used to determine absorbances due to NO_2 and N_2O_4 in the 300 - 400 nm range, and these were subtracted from the measured absorbance to determine that due to N_2O_3. Absorbances determined in this fashion at several wavelengths followed well the linear Beer law dependence on $[N_2O_3]$ over the entire pressure range which could be studied here (0.54 - 6.32 Torr); data for the 300, 310 and 320 nm measurements are shown in Fig. 1. Summarized in Table 1 are the absorption cross sections

$$\sigma_\lambda = \frac{\ln (I_{o\lambda}/I_\lambda)}{[N_2O_3]l} \text{ cm}^2 \text{ molecule}^{-1}$$
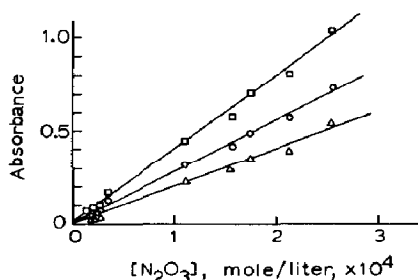
for N_2O_3 at each nanometer in the 300 - 400 nm range.

Fig. 1. Beer's law plots for N_2O_3(g) at some representative wavelengths: □ 300 nm; ○ 310 nm; △ 320 nm.

In the HONO studies HONO was formed from NO_2, NO and H_2O vapors through the equilibrium

$$NO + NO_2 + H_2O \rightleftharpoons 2HONO \tag{11}$$

Mixtures were prepared by adding small amounts of NO_2 and N_2O_4 as before. Then H_2O vapor at its equilibrium pressure at 0 °C was introduced to a calibrated volume in the manifold, and a measured fraction of this was distilled into the cell. This procedure provided the same 1.57 Torr (298 K) initial pressure of H_2O in each run that was made. A measured quantity of nitric oxide gas was then added to the cell as before. The mixture was allowed to warm to room temperature and to equilibrate. Spectra of the mixtures were determined every day for three successive days; they did not change detectably after the first 24 h period, so it seems clear that equilibrium was established in the mixtures used for the HONO absorption cross section measurements in this work. The equilibrium $P(NO_2)$ was measured as before. Using the initial pressures of H_2O and NO, and the measured amount of NO_2 in the equilibrium mixture, the pressures of the other components in the equilibrium mixture were calculated using relations (9), (10) and (12):

$$K_{11} = \exp (-15.56 + 4.73 \times 10^3 T^{-1}) \tag{12}$$

TABLE 1

Dinitrogen trioxide absorption cross sections[†]

Wavelength (nm)	σ (cm^2 molecule^{-1} $\times$ 10^{20})	Wavelength (nm)	σ (cm^2 molecule^{-1} $\times$ 10^{20})	Wavelength (nm)	σ (cm^2 molecule^{-1} $\times$ 10^{20})
300	150	334	68.4	368	29
301	146	335	66.8	369	27
302	141	336	65.7	370	26
303	136	337	63.8	371	26
304	132	338	62.3	372	26
305	128	339	60.3	373	26
306	123	340	58.1	374	26
307	118	341	57.3	375	26
308	113	342	56.1	376	26
309	109	343	55.4	377	27
310	106	344	54.2	378	27
311	101	345	53.5	379	27
312	97.4	346	53.1	380	27
313	94.0	347	52.7	381	25
314	90.9	348	52.3	382	24
315	88.6	349	51.9	383	23
316	85.6	350	51.6	384	21
317	83.3	351	50.4	385	20
318	81.7	352	49.7	386	18
319	79.8	353	48.9	387	17
320	78.3	354	48.1	388	15
321	77.5	355	47.7	389	13
322	76.8	356	47.0	390	12
323	76.4	357	45.8	391	10
324	76.0	358	44.7	392	8.8
325	75.6	359	43.9	393	7.3
326	75.2	360	43.2	394	5.7
327	74.9	361	41.2	895	4.6
328	74.5	362	39.7	396	3.8
329	74.1	363	38.2	397	3
330	73.7	364	36	398	2
331	71.8	365	35	399	1
332	70.7	366	33	400	0
333	69.9	367	31		

[†] $\sigma = \dfrac{\ln(I_o/I)}{[N_2O_3]l}$ cm^2 molecule^{-1}.

Relation (12) was derived by Chan *et al.* [5] from the combined experimental data of Wayne and Yost [20], Waldorf and Babb [21] and Ashmore and Tyler [22]. The JANAF data for the HONO species must be in error since constants derived from these data do not reproduce the experimental equilibrium data [5]. Using these composition data and the known absorption cross sections for NO_2 and N_2O_4 [19] together with our absorption data for N_2O_3 (Table 1), absorbances due to NO_2, N_2O_4 and N_2O_3 were calculated at

1 nm wavelength intervals from 300 to 400 nm. These were subtracted from the total measured absorbance of the equilibrium mixture to obtain the absorbance due to HONO. The fraction of the measured absorbance at 332 and 368 nm which was attributable to HONO was in the range 15 - 67% of the total absorbance measured. The absorbances for HONO followed reasonably well the linear dependence on concentration expected from Beer's law for the very limited range of concentrations which could be determined for this system (1.47 - 3.73 Torr, 25 °C). The absorption cross sections which we have estimated from this study are summarized in Table 2. The accumulated error in these estimates which could result from the absorbance measurements and equilibrium data employed should be less than 10% at the maxima in the HONO absorption spectrum.

The near UV absorption spectrum of N_2O_3 vapor

The absorption cross sections estimated for $N_2O_3(g)$ in the near UV region are presented in Table 1 and plotted in Fig. 2. The continuous nature of the absorption reported previously is confirmed [23]. However, there is a weak but readily discernible structure which can be seen. We attribute this tentatively to the $N_2O_3(g)$. It is not likely that such an effect would result from impurity bands of HONO which may have formed inadvertently from the reaction of the oxides of nitrogen with H_2O impurity released from the cell wall. The amount of such water vapor must be below a few hundred ppm at most, and the equilibrium level of HONO in such a mixture could not create the relatively intense absorption of the broad structure observed here.
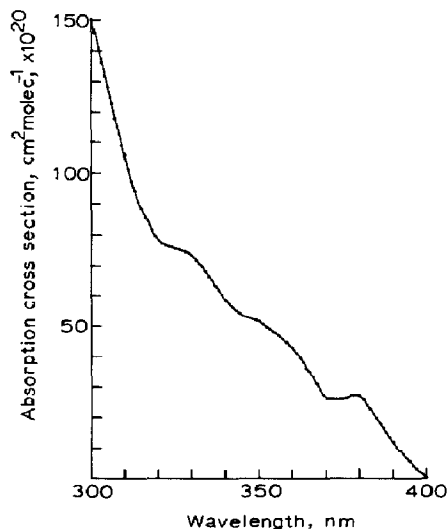

Fig. 2. The absorption cross section for $N_2O_3(g)$ as a function of wavelength.

Furthermore the positions of the strongest HONO bands at 368 and 340 nm are near minima in the broad structure exhibited in Fig. 2. Conceivably the structure could arise owing to faulty correction for NO_2 present in the

TABLE 2

Nitrous acid absorption cross sections[†]

Wavelength (nm)	σ (cm^2 molecule^{-1} $\times$ 10^{20})	Wavelength (nm)	σ (cm^2 molecule^{-1} $\times$ 10^{20})	Wavelength (nm)	σ (cm^2 molecule^{-1} $\times$ 10^{20})
310	0.0	339	16.3	368	45.0
311	0.0	340	10.5	369	29.3
312	0.2	341	8.70	370	11.9
313	0.42	342	33.5	371	9.46
314	0.46	343	20.1	372	8.85
315	0.42	344	10.2	373	7.44
316	0.3	345	8.54	374	4.77
317	0.46	346	8.32	375	2.7
318	3.6	347	8.20	376	1.9
319	6.10	348	7.49	377	1.5
320	2.1	349	7.13	378	1.9
321	4.27	350	6.83	379	5.8
322	4.01	351	17.4	380	7.78
323	3.93	352	11.4	381	11.4
324	4.01	353	37.1	382	14.0
325	4.04	354	49.6	383	17.2
326	3.13	355	24.6	384	19.9
327	4.12	356	11.9	385	19.0
328	7.55	357	9.35	386	11.9
329	6.64	358	7.78	387	5.65
330	7.29	359	7.29	388	3.2
331	8.70	360	6.83	389	1.9
332	13.8	361	6.90	390	1.2
333	5.91	362	7.32	391	0.5
334	5.91	363	9.00	392	0.0
335	6.45	364	12.1	393	0.0
336	5.91	365	13.3	394	0.0
337	4.58	366	21.3	395	0.0
338	19.1	367	35.2	396	0.0

[†] $\sigma = \dfrac{\ln(I_o/I)}{[HONO]l}$ cm^2 molecule^{-1}.

N$_2$O$_3$ mixture, but experiments in which NO$_2$ absorption was matched in the reference beam of the spectrometer also showed this broad structure. We are not aware of any tabular data with which we can compare these cross-section estimates. Johnston and Graham [7] did not publish their measured data for N$_2$O$_3$. Those of Shaw and Vosper [23] were presented in graphical form only, and the scale of the plot chosen makes impossible an accurate reading at the wavelength of most intense absorption in our work (300 nm); however, it appears to be qualitatively consistent with our estimates.

The near UV spectrum of HONO vapor

The absorption cross section data for HONO determined in this study are summarized in Table 2 and plotted in Fig. 3 (the solid curve). These data
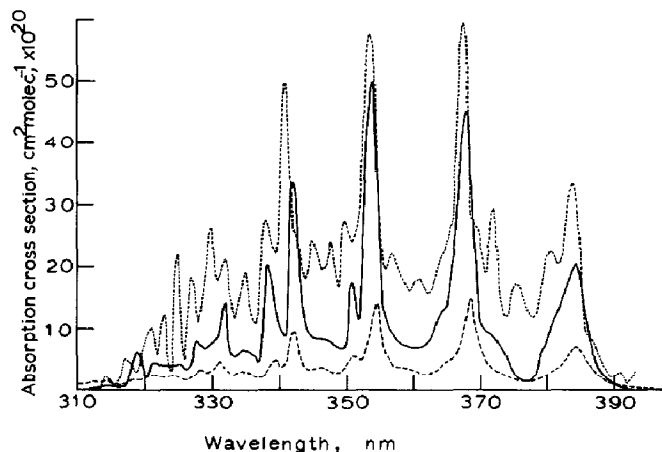
200 200

Fig. 3. The absorption cross section for HONO(g) as a function of wavelength: data from the present work are shown as a solid curve; those of Cox and Derwent [8] and Johnston and Graham [7] are given by the lower and upper broken curves, respectively.

can be compared with those estimated in the studies of Johnston and Graham [7] (the lower broken curve) and Cox and Derwent [8] (the upper broken curve). It is apparent that the magnitude of the cross sections for the peaks in absorption estimated in our work are more nearly equal to those of Cox and Derwent, although the vibrational structure which we observe correlates better with the data of Johnston and Graham [7]. The peaks seen in the Cox and Derwent spectrum near 325, 330, 345, 348, 357, 361, 373, 376, 380 and 391 nm do not appear in our HONO absorption spectrum or in those reported by Johnston and Graham [7] and King and Moule [6]. We noted that maxima occur very near these wavelengths in the spectrum of NO_2 gas [19]. The magnitude of these peaks is within the uncertainty in the HONO cross sections reported by Cox and Derwent. However, if these peaks are real, then it is likely that the Cox and Derwent spectral data for HONO include some uncorrected absorptions from NO_2 impurity in their mixtures. In making the corrections for NO_2 absorption, they employed the Johnston and Graham absorption data for NO_2 which lists only values at wavelength intervals of 5 nm [7]. It seems inevitable that some peak structure of NO_2 must be retained in the corrected spectrum of HONO using this procedure. If one assumes that this is the origin of the difference between our absorption data and those of Cox and Derwent and that they have correctly estimated the concentration of HONO in their mixtures, then we expect the uncorrected NO_2 to be given by

$$[NO_2]_{uncor} \approx [HONO] \ \frac{\sigma'(HONO) - \sigma(HONO)}{\sigma(NO_2)}$$

where $\sigma'(HONO)$ is the apparent absorption cross section observed by Cox and Derwent, and $\sigma(HONO)$ and $\sigma(NO_2)$ are the correct values for HONO and NO_2, respectively. Using the Cox and Derwent data from 345, 348, 357, 361, 372, 376 and 380 nm and assuming our $\sigma(HONO)$ values to be correct, we

estimate $[NO_2]_{uncor}/[HONO] \approx 0.24 \pm 0.07$ in the Cox and Derwent experiments. Of course the net effect of having uncorrected absorption due to NO_2 present is to raise the $\sigma(HONO)$ estimate. It seems likely to us that this may have occurred in the experiments of Cox and Derwent.

The seemingly low values of absorption cross sections for HONO derived by Johnston and Graham may reflect non-equilibrium levels of HONO in their reaction mixtures as Cox and Derwent have suggested, since reactions (3) and (4) are relatively slow in the NO_2, NO, H_2O and He gas mixtures employed. These workers do not describe the time dependence of the growth of HONO observed nor the period of delay before final measurements were made, so such a suggestion must remain as conjecture. The ratio of peak to valley cross sections in the three data sets now available for HONO are inconsistent. Thus $\sigma_{354}/\sigma_{360} = 3.74, 3.29$ and 7.26 from the data of Johnston and Graham [7], Cox and Derwent [8] and our data, respectively. Conceivably this difference may have resulted from an overcorrection for NO_2 in our study. However, if this were the case one should observe minima in the calculated spectrum of HONO which would correspond to the NO_2 peaks. This is not observed. It seems more likely to us that the data of the other workers were undercorrected for the presence of NO_2.

A test of the reliability of the HONO absorption cross section data can be made using rate data derived in our large photochemical reactor system. The UV light which bathes the cell contents rather uniformly mimics quite well the ground level solar flux both in intensity and wavelength distribution in the 2900 - 4100 Å region. FTS IR spectrometric analysis of reactants and products can give a fairly continuous record of the chemistry which occurs in the reactor. The apparent first order rate constant for reaction (7) was determined in a series of experiments employing low concentrations of HONO in 700 Torr of air and in mixtures with small quantities of added CO, NO and NO_2 in 700 Torr of air [24]. Rate data on reaction (13) were obtained in another series of experiments at low concentrations of NO_2 carried out both in the absence and in the presence of 700 Torr of air.

$$HONO + h\nu \rightarrow HO + NO \qquad (7)$$

$$NO_2 + h\nu \rightarrow O + NO \qquad (13)$$

The kinetic treatment of these data gave $k_7 \approx 0.11$ and $k_{13} \approx 0.60$ min^{-1} [13]. The relative light intensity *versus* wavelength distribution function $F(\lambda)$ for the UV light within the cell was determined using an absolute spectrofluorimeter as detector. These data were coupled with our present $\sigma(HONO)(\lambda)$ estimates, the $\sigma(NO_2)(\lambda)$ data of Bass *et al.* [19], primary quantum yield data $\phi_{13}(\lambda)$ of Jones and Bayes [24] for (13) and the assumption that $\phi_7 = 1$ at all HONO absorbing wavelengths in the 290 - 410 nm range [8] to derive the theoretically expected relative rates of reactions (7) and (13) in our photochemical reactor:

$$\frac{R_7}{R_{13}} = \frac{\int \sigma(HONO)(\lambda) \, F(\lambda) \, \phi_7(\lambda) \, d\lambda}{\int \sigma(NO_2)(\lambda) \, F(\lambda) \, \phi_{13}(\lambda) \, d\lambda} \qquad (14)$$

Using relation (14) and integrating over the 290 - 410 nm range of non-zero values, we obtained $R_7/R_{13} \approx 0.18 \pm 0.02$. This checks well with the ratio of the independently estimated experimental rates: $R_7/R_{13} \approx 0.11/0.60 \approx 0.18 \pm 0.04$. Thus some support is provided for the accuracy of the present HONO cross-section data and the conclusion of Cox and Derwent that $\phi_7 \approx 1.0$ within the first absorption band of HONO. If the $\sigma(HONO)$ values of Johnston and Graham are used in relation (14), we obtain $R_7/R_{13} \approx 0.065$; use of the Cox and Derwent estimates of $\sigma(HONO)$ yields $R_7/R_{13} \approx 0.32$.

We feel that our present estimates of the absorption cross sections of HONO are the most reliable of those available today, and we recommend their use in the modeling of the trophospheric chemistry. We may combine our $\sigma(HONO)$ values with Peterson's recent estimates of the flux of solar radiation at ground level [25] to derive new theoretical estimates of k_6 applicable for the lower troposphere at various solar zenith angles. These estimates are shown in Fig. 4 for the choice of zero surface albedo. They may be increased by the appropriate reflection factor which describes best the properties of the earth's surface at the point of interest.
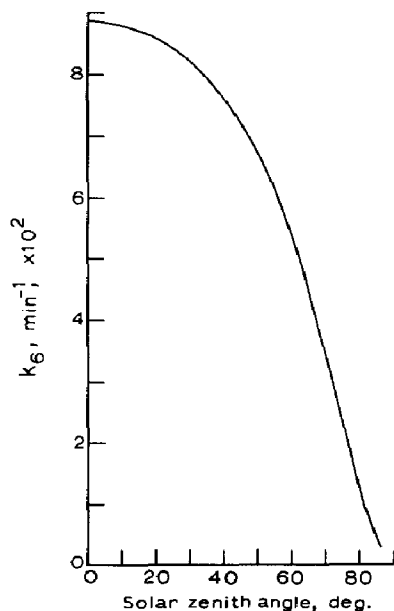

Fig. 4. Estimated first order rate constants for HONO(g) photolysis in sunlight, HONO + sunlight → HO + NO; the data are calculated for sea level and the surface albedo equals zero for various solar zenith angles; actinic flux data from Peterson [25].

The unambiguous detection of HONO in ambient air has not yet been accomplished to our knowledge. Simulations using these estimates suggest that, for a typical NO_x–RH-polluted sunlight-irradiated atmosphere, the levels of HONO, controlled largely by reactions (1) - (6), which are expected to be present near ground level should be in the ppb range. Obviously a sensitive detector system will be necessary to identify HONO successfully in the ambient air.

Acknowledgment

References

1 T. Nash, Tellus, 26 (1974) 175 - 179
2 T. Nash, Am. Occup. Hyg., 11 (1968) 235 - 239.
3 K. L. Demerjian, J. A. Kerr and J. G. Calvert, Adv. Environ. Sci. Technol., 4 (1974) 1 - 262.
4 J. G. Calvert and R. D. McQuigg, Int. J. Chem. Kinet., Symp., 1 (1975) 113 - 154.
5 W. H. Chan, R. J. Nordstrom, J. G. Calvert and J. H. Shaw, Environ. Sci. Technol., 10 (1976) 674 - 682.
6 G. W. King and D. Moule, Can. J. Chem., 40 (1962) 2057 - 2065.
7 H. S. Johnston and R. Graham, Can. J. Chem., 52 (1974) 1415 - 1423.
8 R. A. Cox and R. G. Derwent, J. Photochem., 6 (1976/77) 23 - 34.
9 R. A. Cox, J. Photochem., 3 (1974) 175 - 188.
10 R. A. Cox, J. Photochem., 3 (1974) 291 - 304.
11 R. A. Cox, Int. J. Chem. Kinet., Symp., 1 (1975) 379 - 398.
12 W. H. Chan, W. M. Uselman, J. G. Calvert and J. H. Shaw, Chem. Phys. Lett., 45 (1977) 240 - 244.
13 S. Z. Levine, W. M. Uselman, W. H. Chan, J. G. Calvert and J. H. Shaw, Chem. Phys. Lett., 48 (1977) 528 - 535.
14 T. C. Hall, Jr., and F. E. Blacet, J. Chem. Phys., 20 (1952) 1745 - 1749.
15 JANAF Thermodynamic Tables, 2nd edn., Nat. Stand. Ref. Data Ser., Nat. Bur. Stand., 37 (1971).
16 F. H. Verhoek and F. Daniels, J. Am. Chem. Soc., 53 (1931) 1250 - 1263.
17 E. W. Kaiser and C. H. Wu, J. Phys. Chem., 81 (1977) 187 - 190.
18 E. R. Beatte and S. W. Bell, J. Chem. Soc., (1957) 1681 - 1686.
19 A. M. Bass, A. E. Ledford and A. H. Laufer, J. Res. Nat. Bur. Stand., Sect. A, 80A (1976) 143 - 166.
20 L. G. Wayne and D. M. Yost, J. Chem. Phys., 19 (1951) 41 - 47.
21 D. M. Waldorf and A. L. Babb, J. Chem. Phys., 39 (1963) 432 - 435; 40 (1964) 1165.
22 P. G. Ashmore and B. J. Tyler, J. Chem. Soc., (1961) 1017 - 1021.
23 A. W. Shaw and A. J. Vosper, J. Chem. Soc. Dalton Trans., (1972) 961 - 964.
24 I. T. N. Jones and K. D. Bayes, Chem. Phys. Lett., 11 (1971) 163 - 166.
25 J. T. Peterson, Calculated actinic fluxes (290 - 700 nm) for air pollution photochemical applications, Rep. EPA-600/4-76-025, Environmental Protection Agency, Research Triangle Park, N.C., June 1976.